BOND-SLIP MODELS FOR DOUBLE STRAP JOINTS STRENGTHENED BY CFRP

Sabrina Fawzia[1*], Xiao-Ling Zhao[2], Riadh Al-Mahaidi[2]
[1]School of Urban development, Queensland University of Technology, Brisbane Queensland 4000, Australia, email: sabrina.fawzia@qut.edu.au
[2]Department of Civil Engineering, Monash University, Clayton, Victoria 3800, Australia,
email: ZXL@eng.monash.edu.au; al-mahaidi@eng.monash.edu.au
(*corresponding author: sabrina.fawzia@qut.edu.au)

ABSTRACT

This paper presents the results of a series of tension tests on CFRP bonded steel plate double strap joints. The main aim of this research is to provide detailed understanding of bond characteristics using experimental and numerical analysis of strengthened double strap joints under tension. A parametric study has been performed by numerical modelling with the variables of CFRP bond lengths, adhesive maximum strain and adhesive layer thicknesses. Finally, bond-slip models are proposed for three different types of adhesives within the range of the parametric study.

Keywords: Composite materials, CFRP, Bond-slip, Double strap joint, Steel, Strengthening.

Notations

l_1 = Shorter bond length

l_2 = Longer bond length

P_{ult} = Ultimate load

τ_f = Adhesive maximum shear stress (MPa)

δ_1 = Initial slip (mm)

δ_f = Maximum slip (mm)

t_a = Adhesive layer thickness (mm)

σ_a =Adhesive tensile strength (MPa)

t_s =Steel plate thickness,

t_{CFRP} =CFRP sheet thickness

T =Total thickness of the specimen,

n=number of layers

1 INTRODUCTION

Advanced composite materials have recently found their way into civil engineering infrastructure. The evolution of carbon fibre reinforced polymer (CFRP) technologies and the versatility of their applications in civil engineering constructions necessitate comprehensive and reliable codes of practice. To enable the use of CFRP composites for strengthening steel structures, an understanding of bonding mechanisms is therefore essential. Bond strength is usually used to determine bond performance. Bond strength can be defined as the ratio of maximum load and interfacial area. However, a local bond-slip relationship is independent of geometric conditions, and therefore a local bond-slip model may be appropriate to measure bond performance. While a great deal of research has been carried out on bond-slip relationships of CFRP sheet/plate bonded to concrete joints [1-9], research on CFRP plate/sheet to steel bonded joints is limited [10-15]. Previous research [10] showed a significant strength increase by using CFRP–epoxy strengthening technique. In this research a theoretical model was developed to estimate the load carrying capacity of butt-welded very high strength steel tubes strengthened using CFRP. In previous papers [11-14], the authors showed significant strength enhancement of CFRP strengthened steel plate and steel tube by experimental, theoretical and finite element analysis. None of the above research developed bond slip relationship. Xia and Teng [15] have reported results of bond slip relationship for CFRP laminate to steel bonded joints. Their research identified a simple bi-linear bond-slip relationship which is shown in Figure

1. This bond-slip plot has a linear ascending branch followed by a linear descending branch. The schematic view presented in Figure 1 which can be defined by three parameters τ_f, δ_1 and δ_f where

τ_f = Adhesive maximum shear stress (MPa), δ_1 = Initial slip (mm) and δ_f = Maximum slip (mm). The initial stiffness of the bond-slip response is high, representing a linear elastic state. Initiation of the interfacial softening stage means that load continues to increase as the length of the softening zone increases. The ultimate load is first attained at the end of this stage and starts propagation of debonding. However, there is no research on bond-slip models for CFRP sheet bonded to steel structures.

This paper reports an experimental investigation to study local bond-slip relationships for CFRP sheets bonded to steel structures by the wet lay up method. Strain distributions measured by foil strain gauges for different adhesives are used to quantify shear stress and slip. The possibility of finding local bond-slip relationships using large bond length (e.g. at least twice the effective bond length) is strictly related to the consideration of the distribution of slip and shear stress along the bond length. Finally a bilinear bond-slip model is proposed based on the results from experimental and numerical studies.

2 EXPERIMENTAL PROCEDURE

In order to determine shear stress and slip relationship by using strain distributions, a series of double strap joint specimens were tested using a 500kN capacity Baldwin universal testing machine. A total of twenty seven CFRP/steel joint specimens were designed to test under tension. For each of the joints, two pieces of steel plates, 400mm long, 50mm wide and 6 or 10mm thick, were used. A schematic view of a specimen is shown in Figure 2. In the specimens, length l_1 was always kept less than

l_2 to ensure that the failure occurred on one end only. Foil strain gauges (VMMCEA-13-240UZ-120) were used in the experiments placing them on the shorter bond length to capture longitudinal strain distribution. Figure 3 shows the strain gauge positions of different series of specimens. The dark colour represents the CFRP bond length. Details of material properties, specimen preparation and test parameters considered in the experiments are described in the following sections.

2.1 Material Properties

The measured properties of normal and high modulus CFRP's tensile strength and strain are 2675 MPa and 1.2% and 1175 MPa and 0.2%, respectively. The tensile strength and strain of adhesives Araldite 420, MBrace saturant and Sikadur 30 is 28.6 MPa and 2.4%; 24.8MPa and 1.46%; 24MPa and 0.3%, respectively. More details of material property measurement can be found in Fawzia [11].

2.2 Specimen Procedures

The steel plates were grinded by angle grinder in the area to be bonded to ensure better mechanical interlocking. The surfaces were cleaned with acetone to remove grease, oil and rust. A small amount of adhesive was applied first at the cross-sectional surfaces of the steel plate. Two plates were bonded together. The jointed plate was cured for 24 hours. Adhesive was then applied on the steel plate uniformly along the bond length of the steel plate. Then the first layer of CFRP sheet was placed on top of the adhesive. Every effort has been made to ensure uniform adhesive layer thickness in the specimen. A roller was applied on the specimen surface to squeeze out excess adhesives and maintain uniform thickness along entire bond length. It needs to be mentioned here that it is extremely difficult to obtain 100% uniform adhesive layer thickness. However, average adhesive thickness was calculated using the method described in section 5. Following the above procedures, two more layers

of CFRP sheets were applied on top of the first layer and the specimen was cured for a few days. After that, three layers of CFRP were applied on the other side of the steel plate following the same procedure. The specimens were then cured for 7 days at ambient temperature and post cured for one day at 70^{o}C.

2.3 Test Parameters

A number of parameters have been used in the testing series to investigate their influence on the performance of the joint. The parameters were the types of CFRP (normal modulus and high modulus CFRP), types of adhesives (Araldite 420, MBrace Saturant and Sikadur 30), number of CFRP layers (3 and 5), bond length (80 to 250mm) and steel thickness (6 and 10mm). The configurations of the five series are given in Table 1.

3 TEST RESULTS AND FAILURE MODE

Results from the double strap shear test are presented in Table 2. In the first column of Table 2, N stands for normal modulus CFRP sheet, H stands for high modulus CFRP sheet, A stands for Araldite 420, M stands for MBrace saturant, S stands for Sikadur 30 and ‘a’,’b’,’c’ and ‘d’ indicate four specimens with identical bond lengths. In most cases, specimens with all three types of adhesives exhibited combined failure modes, which is a combination of steel adhesive interface debonding and CFRP delamination. More details about this failure mode can be found in Zhao and Zhang [16]. Figure 4 shows the failure mode achieved for three different adhesives. Preliminary tests [12] showed that high modulus CFRP experienced CFRP rupture failure with 3 layers of CFRP. In the present test series five layers of high modulus CFRP joint was used to check if interfacial debonding or bond failure (instead of CFRP failure) would occur. However, CFRP rupture failure occurred even with five layers of CFRP.

In the present study, the average experimental shear stress was calculated from the readings of strain gauges mounted on the top surface of the CFRP sheet. The calculated shear stress distributions along the distance away from the "steel joint" are shown in Figure 5 for a typical specimen of Sikadur 30 adhesive at different load levels. Araldite 420 and Mbrace saturant adhesive specimens also showed similar shear stress distribution.

It can be seen from the figure that the shear stress is highest at the loaded end from load level 28 to 60 kN load level . But at 68 kN load level shear stress decreases at the loaded edge. When the peak shear stress starts decreasing at the loaded edge and moves away from the joint, the linear stage of the load-displacement curve ends, and the softening stage starts. When the shear stress at the loaded end reduces to zero, the ultimate load of the specimen is reached which is 76kN. These stages of development are the same as those described for FRP-to-concrete bonded joints in Yuan et al [6].

4 FINITE ELEMENT ANALYSIS

In this study, Finite element method (FEM) is used to perform tensile testing simulations by nonlinear static analysis on double strap joints bonded by adhesive and CFRP sheet material. Special attention needs to be paid when joining two different materials, in this particular case adhesive bonding between steel and CFRP. The simulation was implemented using commercially available finite element analysis software Strand7. Details of FE analysis can be found in Fawzia et al [12]. Strand 7 is a general purpose finite element software. Three dimentional model has been constructed with 8-node brick elements. To model the adhesive layer accordingly, this layer was assumed to have uniform thickness throughout.

Since the failure mode is debonding and the adhesive layer is the critical region, it is important to show the shear stress distribution along the adhesive layer. Therefore the

shear stress is calculated at the same location where the experimental shear stress is obtained along the bonded length. Figure 6 shows a typical shear stress distribution along the distance away from the "steel joint" at the adhesive layer for two different applied loads. The tensile load is applied at both ends of the specimen. The specimen consists of two steel plate bonded together and therefore the joint location shown in Figure 2 is the loaded edge. The contour representing the maximum shear stress is given in Figure 6.

5 BOND-SLIP RELATIONSHIP

Local slips are calculated by integrating measured strain distribution along the bond length. This local slip is the relative displacement between the CFRP sheet and the steel plate. Calculated shear stresses and slips are combined to obtain the local shear stress-slip curves. The local shear stress slip relationship is reasonably consistent between different locations on the same specimen [15]. Therefore the model presented here shows maximum shear stress slip relationships from different locations on the same specimen and compares the same results by numerical modelling. The shear stress and slip relationships have been studied experimentally for three types of adhesives. Figures 7-9 present comparisons of the shear stress slip model of 200 mm bond length of experimental specimens with the finite element model for three different types of adhesives, Araldite 420, MBrace saturant and Sikadur 30. The measured average adhesive thickness is 0.47mm. Therefore the thickness of adhesive layer can be determined as follows as Equation 1

$$t_a = \frac{\frac{1}{2}(T - t_s)}{n} - t_{CFRP} \tag{1}$$

Where, t_a = Adhesive layers thickness, T =Total thickness of the specimen, t_s =Steel plate thickness, t_{CFRP} =CFRP sheet thickness and n=number of layers

The average adhesive thickness has been measured by calculating thickness of three different places and finally averaged them. The numerical model is in good agreement with the experimental results.

The average value of corresponding experimental and FE results have been adopted as the value for maximum shear stress, initial slip and maximum slip. With reference to Figures 7, 8 and 9 the results for maximum shear stress, slip at maximum shear stress (initial slip) and maximum slip of the Araldite 420 specimen, MBrace Saturant specimen and Sikador 30 is presented in Table 3. Araldite 420 and MBrace saturant adhesive show similar results for initial and maximum slip although the maximum shear stresses are different. Sikadur 30 shows smaller initial and maximum slip compared to other adhesives because of their high modulus of elasticity. The shear stress is highest for Araldite 420 and lowest for Sikadur 30 adhesive.

Figure 1 shows the bond-slip relationship for CFRP laminate strengthened steel plate [15]. The bond-slip curves in Figures 7 to 9 for CFRP sheet strengthened steel plate are similar to that shown in Figure 1, although different values of maximum shear stress, initial slip and maximum slip are expected. In the sections to follow, a parametric study is described using the FE models.

6 PARAMETRIC STUDY

A parametric study has been conducted using finite element analysis. The main parameters studied are CFRP bond length, adhesive maximum strain and adhesive layer thickness.

6.1 CFRP Bond Length

The full distribution of the bond slip model can be achieved by the bond length which is at least twice the effective bond length. Finite element analysis has been carried out for bond lengths of 150, 200, 250 and 400mm for all types of adhesives. All types of

adhesive specimens exhibited similar behaviour. Figure 10 gives the results for Araldite 420 adhesive. It can be seen that the bond-slip model is not affected by the bond length, even up to five times the effective bond length.

6.2 Adhesive maximum strain

An important property of an adhesive is its maximum strain value. Figure 11 shows the effect of different strain values at the same tensile strength level. Two models have been run with the same tensile strength value but different maximum strain values. The tensile strength and maximum strain for one of the models is 30 MPa and 3% strain, while the other model uses 30 MPa and 5% strain. The results show that the initial slip and shear stress are the same for both models, but the maximum slip is higher for the higher strain value, although not significantly.

6.3 Adhesive Thickness

The thickness of the adhesive layer has a significant effect on the failure mode for CFRP laminate strengthening [15]. Since CFRP sheets have been used in this study, it was very difficult to maintain uniform adhesive thickness along the bond line. A parametric study has been conducted to investigate the effect of bond line thickness. Figure 12 shows the results from three different models using 0.1, 0.47 and 1mm adhesive thickness with 30 MPa tensile strength and 3% maximum strain. Results show that the slip is directly proportional to adhesive thickness. Three more FE models have been analysed with the same adhesive thicknesses of 0.1, 0.47 and 1 mm but with 5% maximum strain. Figure 13 shows the relationships of initial and maximum slip according to the adhesive thickness of the model. The variations of initial and maximum slip with different adhesive thicknesses are similar for all three models with 3% and 5% maximum strain. Results also show that both initial and maximum slip increase with the increase of adhesive thickness.

7 LINEAR BOND-SLIP MODEL APPROXIMATION

Bond length greater than the effective bond length has nearly no influence on maximum shear stress τ_f, initial slip δ_1 and maximum slip δ_f of the bond-slip model. The maximum strain has influence on the δ_f value. Based on all parametric studies, the three values of maximum shear stress τ_f, initial slip δ_1 and maximum slip δ_f from Figure 1 of the bilinear bond-slip model can be approximated as follows:

$$\tau_f = \sigma_a \tag{1.1}$$

$$\delta_1 = \frac{t_a}{10} \tag{1.2}$$

$$\delta_f = \frac{t_a}{4} \text{ for } t_a = 0.1 \text{ to } 0.5 \text{ mm} \tag{1.3(a)}$$

$$\delta_f = 0.125 + \frac{t_a - 0.5}{10} \text{ for } t_a = 0.5 \text{ to } 1\text{mm} \tag{1.3(b)}$$

Equations 1.2 and 1.3 in Figure 13 represent the relationship between slip and adhesive thicknesses.

8 SUMMARY

In this paper the test results from double strap joint specimens under tension were presented. CFRP sheet was used with three different types of adhesives. The investigated variables were CFRP bond lengths, adhesive maximum strain and adhesive thickness. The findings from the experimental and parametric studies are summarised as follows:

- The shear stress decreases from the loaded edge to the distance away from the joint.
- The bond-slip model is not affected by the bond length beyond the effective bond length.

- The peak strain assumed in the stress-strain plots of the adhesives has a direct influence on the maximum slip. The peak strain values have no influence on the maximum shear stress and initial slip values.
- The thickness of adhesive layer has significant effects on the bond-slip model. Both initial and maximum slip increase as the adhesive thickness increases.
- The expressions of the three key parameters of bond-slip models, maximum shear stress τ_f, initial slip δ_1 and maximum slip δ_f are proposed within the range of variables used in the parametric study.

ACKNOWLEDGEMENT

This project was sponsored by the Australian Research Council through an ARC Discovery Grant. The authors would like to thank Mr. Long Goh and Mr. Kevin Nievaart for their assistance in carrying out the tests.

REFERENCES

1. Focacci F, Nanni A, Bakis CE. Local bond-slip relationship for FRP reinforcement in concrete. Journal of Composite for Construction ASCE 2000; 4(1):24-31.

2. Chen JF, Teng JG. Anchorage strength models for FRP and steel plates bonded to concrete. Journal of Structural Engineering ASCE 2001; 127(7):784-791.

3. Nakaba K, Kanakubo T, Furuta T, Yoshizawa H. Bond-behaviour between fiber-reinforced polymer laminates and concrete. ACI Structural Journal 2001; 98(3):359-367.

4. Teng JG, Chen JF, Smith ST, Lam L. FRP strengthened RC structures. John Willey & Sons Ltd, West Sussex, UK, 2002.

5. Lee TK. Shear strength of reinforced concrete T-beams strengthened using carbon fibre reinforced polymer (CFRP) laminates. Ph.D Thesis, Monash University, Melbourne, Australia 2003.

6. Yuan H, Teng JG, Seracino R, Wu ZS, Yao J. Full-range behaviour of FRP-to-concrete bonded joints. Engineering Structures 2004; 26(5):553-565.

7. Dai J, Ueda T, Sato Y. Development of the nonlinear bond stress–slip model of fiber reinforced plastics sheet–concrete interfaces with a simple method. Journal of Composites for Construction 2005; 9(1):52-62.

8. Lu XZ, Teng JG, Ye LP, Jiang JJ. Bond-slip models for FRP sheets/plates bonded to concrete. Engineering Structures 2005; 27(6):920-937.

9. Pham H, Al-Mahaidi R. Modelling of CFRP-concrete shear-lap tests. Construction and Building Materials 2007; 21(4):727–735.

10. Jiao H, Zhao XL. CFRP strengthened butt-welded very high strength (VHS) circular steel tubes. Thin-Walled Structures 2004; 42(7): 963-978.

11. Fawzia S, Zhao XL, Al-Mahaidi R, Rizkalla S. Investigation into the bond between CFRP and steel tubes. The Second International Conference on FRP Composites in Civil Engineering (CICE2004), Adelaide, 8-10 December 2004. p. 733-739.

12. Fawzia S, Zhao XL, Al-Mahaidi R, Rizkalla S. Bond Characteristics between CFRP and steel plates in double strap joints. Advanced Steel Construction - an International Journal 2005; 1(2):17-28.

13. Fawzia S, Al-Mahaidi R, Zhao XL. Experimental and Finite Element Analysis of a Double Lap Shear Connection between Steel Plates and CFRP. Composite Structures 2006; 75(1-4):156-162.

14. Fawzia S, Al-Mahaidi R, Zhao XL. Strengthening of circular hollow steel tubular sections using high modulus CFRP sheets. Construction and Building Materials 2007; 21(4): 839-847.

15. Xia SH, Teng JG. Behaviour of FRP-to-steel bonded joints. Proceedings of the International Symposium on Bond Behaviour of FRP in Structures (BBFS 2005), Hong Kong, 2005. p. 419-426.

16. Zhao XL, Zhang L. State-of-the-art review on FRP strengthened steel structures. Engineering Structures 2007; 29(8):1808-1823.

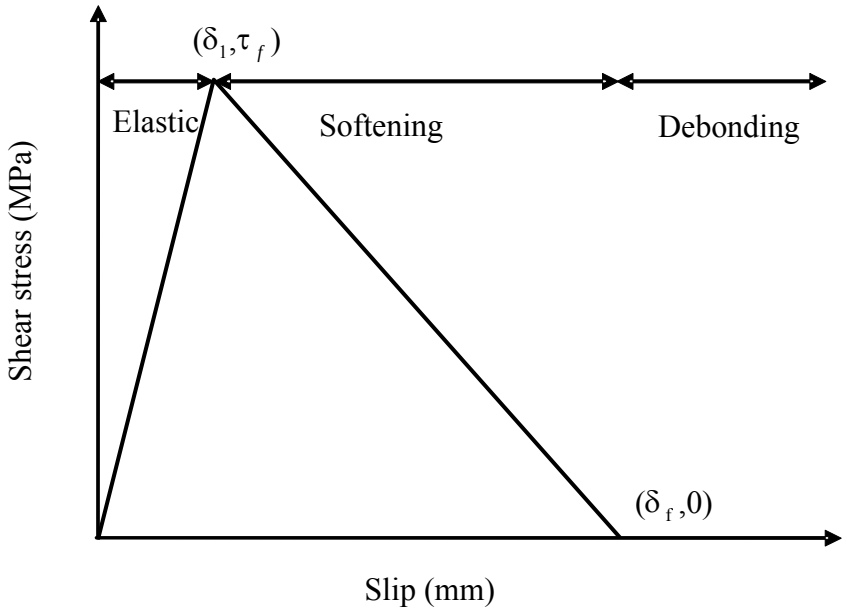

Figure 1 Bilinear bond-slip model approximation for CFRP plate [15]

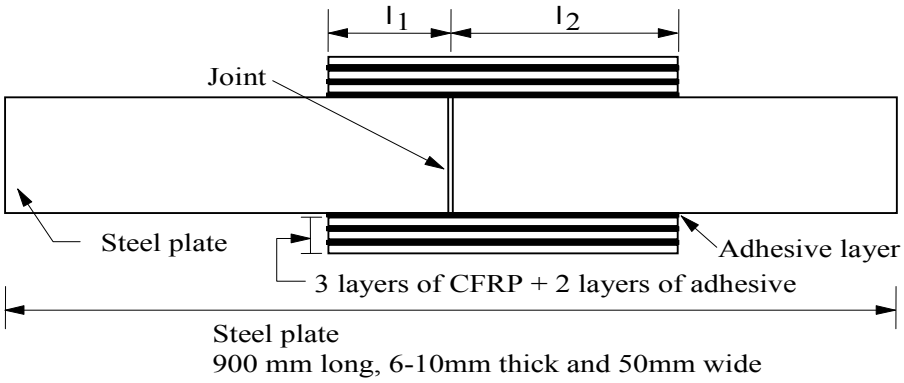

Figure 2 Schematic view of the specimen using CFRP sheet (not to scale)

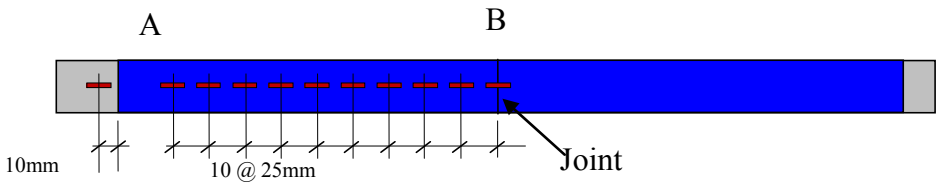

(a) First series, frontside plan

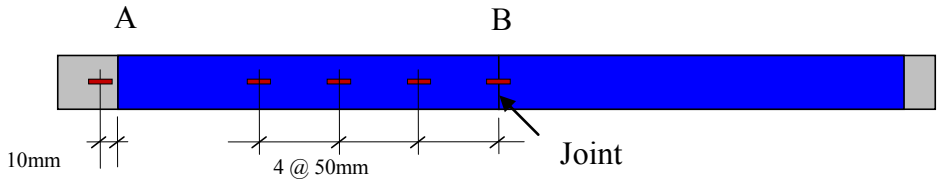

(b) First series, backside plan

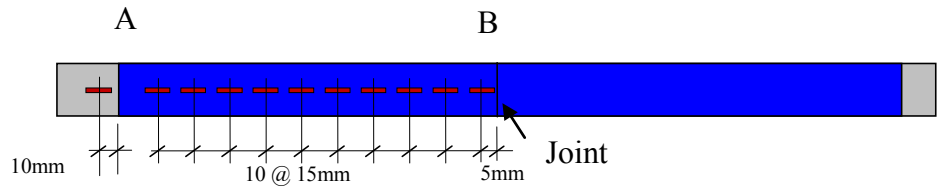

(c) Second, third, fourth and fifth series, frontside plan

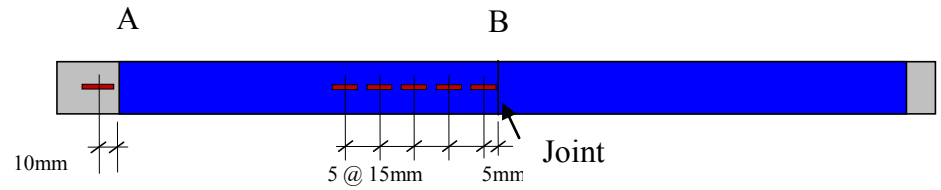

(d) Second, third, fourth and fifth series, backside plan

Figure 3 Strain gauge positions for all specimens (not to scale)

(a) Araldite 420

(b) Mbrace saturant

(c) Sikadur 30

Figure 4 Failure mode

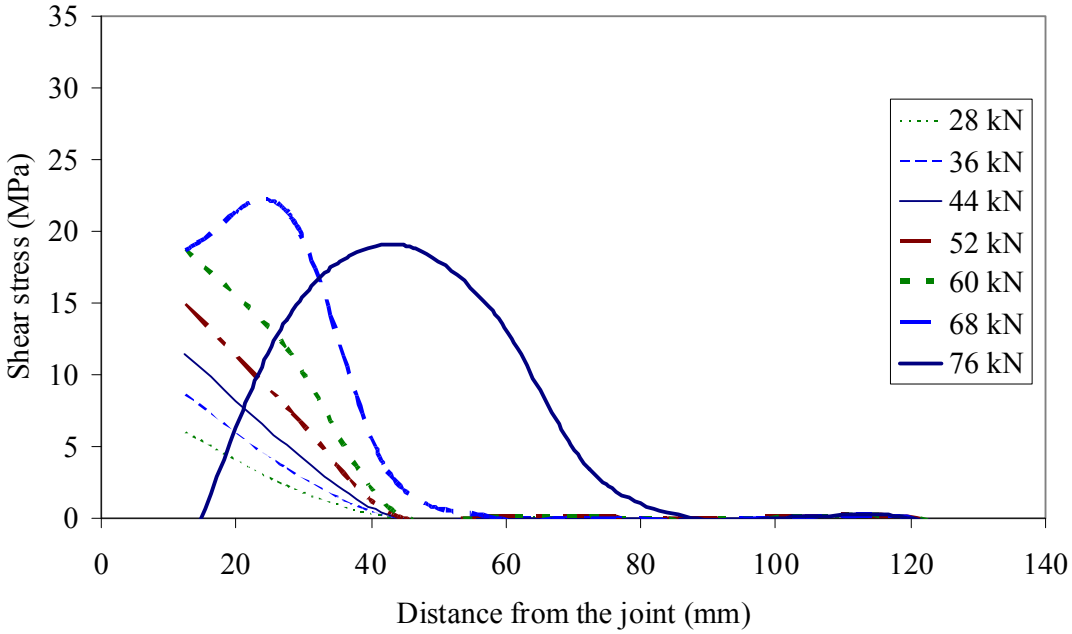

Figure 5 Shear stress distribution (specimen with Sikadur 30 and bond length of 200mm)

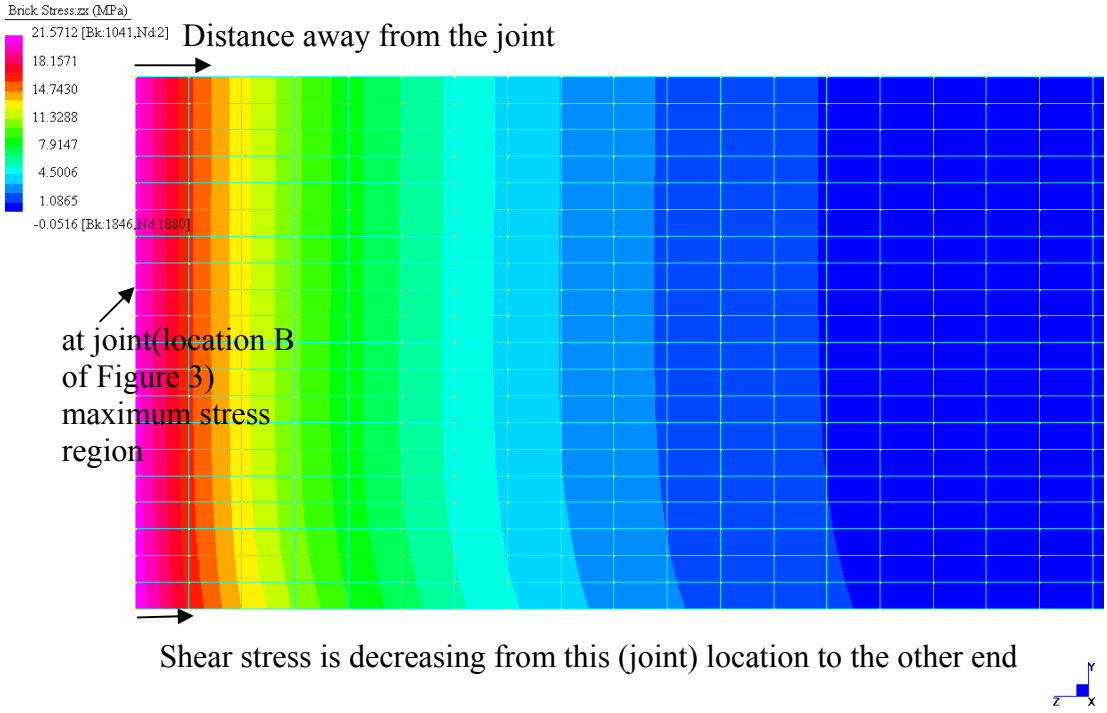

(a) at 60 kN load level

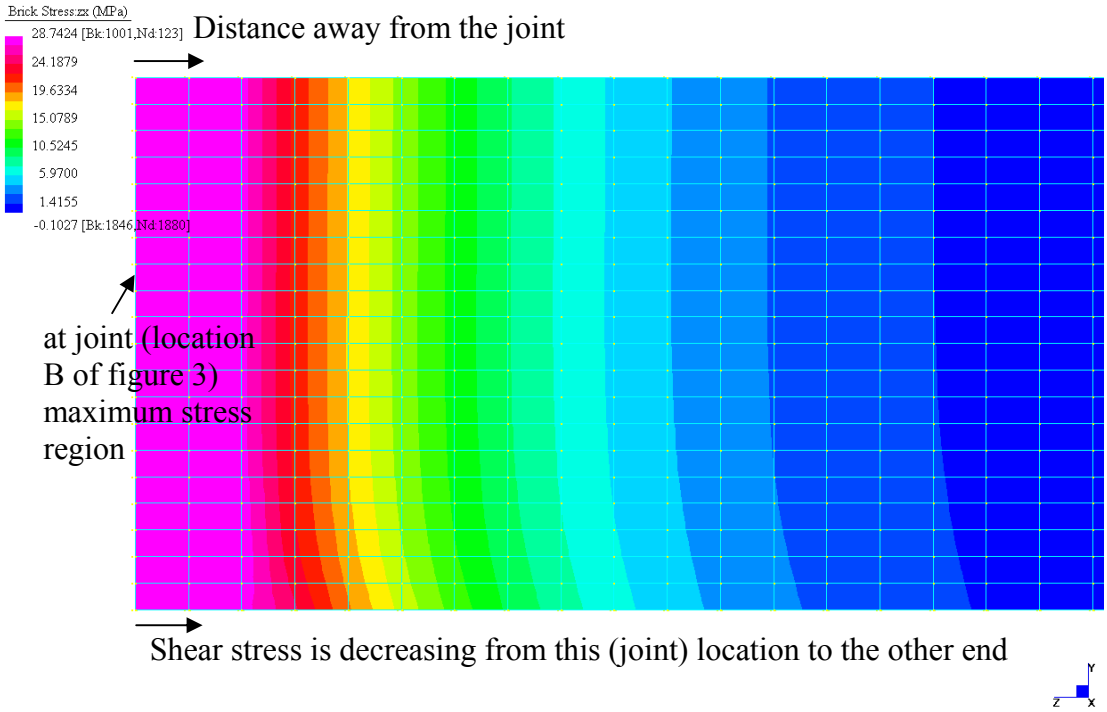

(b) at 80 kN load level

Figure 6 Shear stress distributions (adhesive layer) for a typical specimen at the location of B(joint) towards A of Figure 3

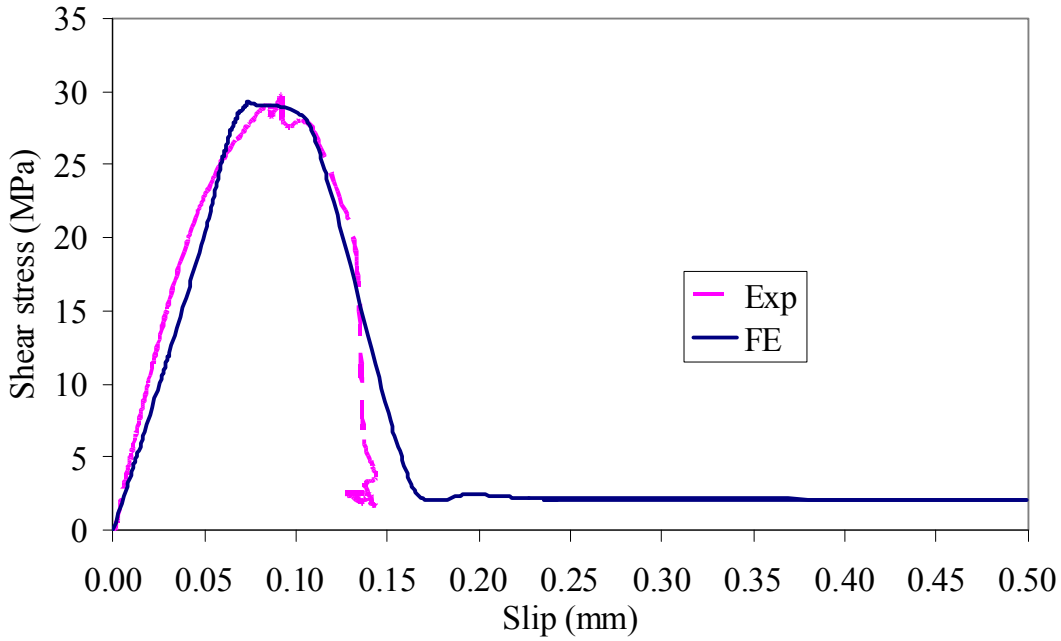

Figure 7 Comparison of the shear stress and slip relationships of experimental Results and FE for Araldite 420 specimen

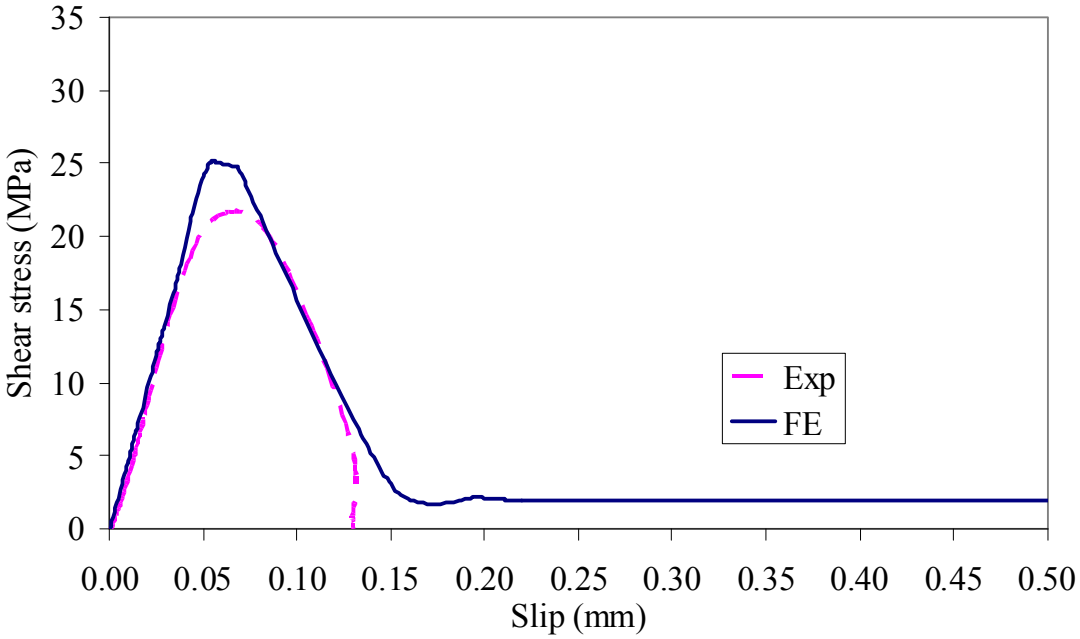

Figure 8 Comparison of the shear stress and slip relationships of experimental results and FE for MBrace saturant specimen

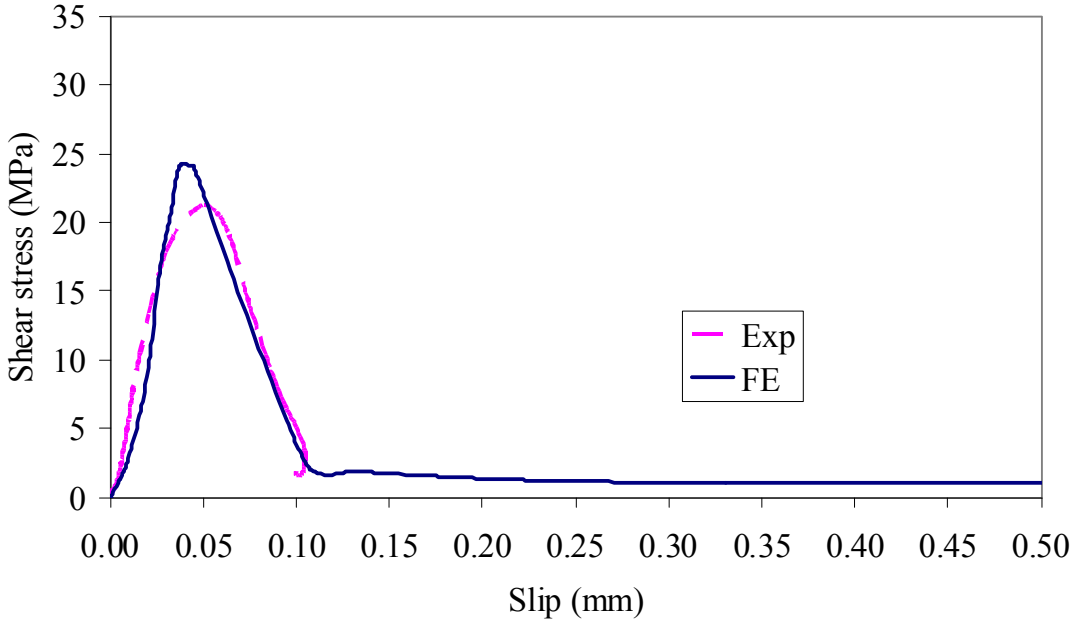

Figure 9 Comparison of the shear stress and slip relationships of experimental results and FE for Sikadur 30 specimen

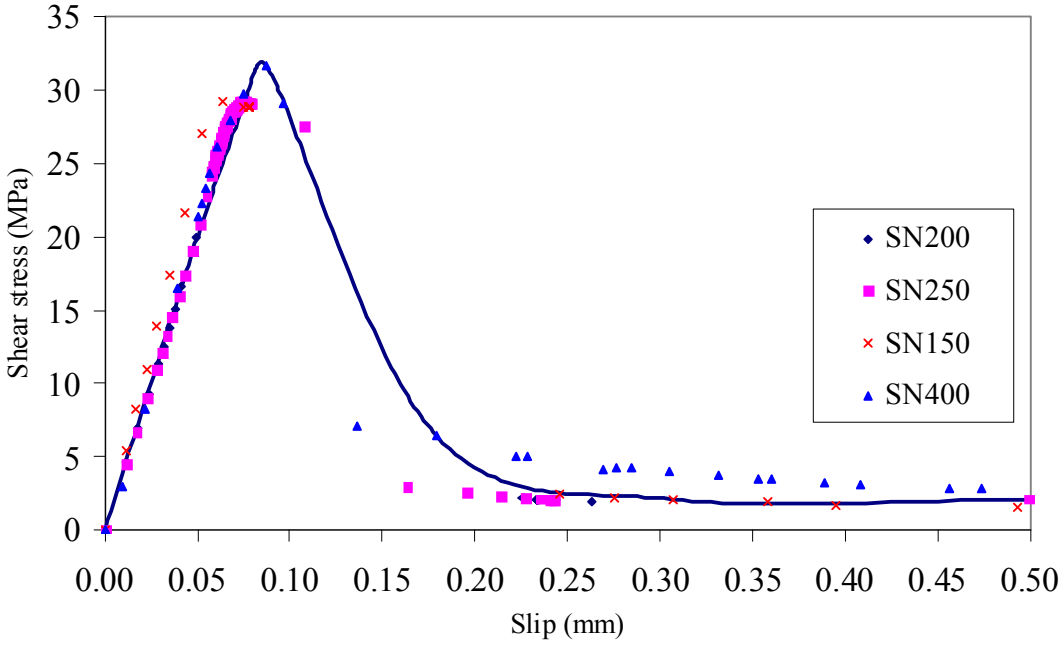

Figure 10 Bond-slip models for different bond lengths of Araldite 420 specimen

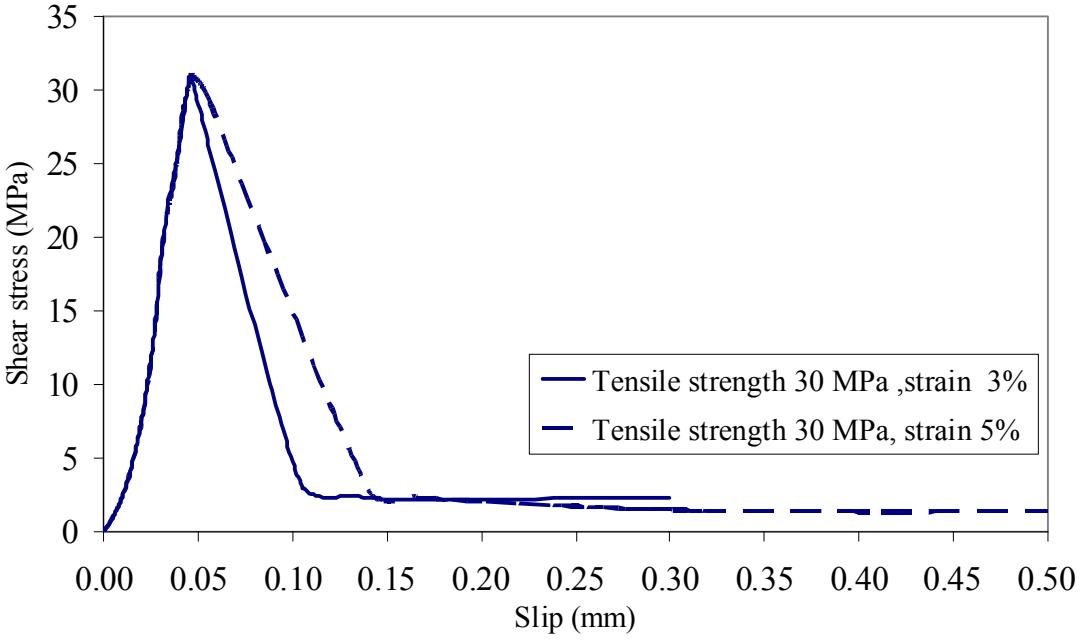

Figure 11 Effect of different strain values in bond-slip model

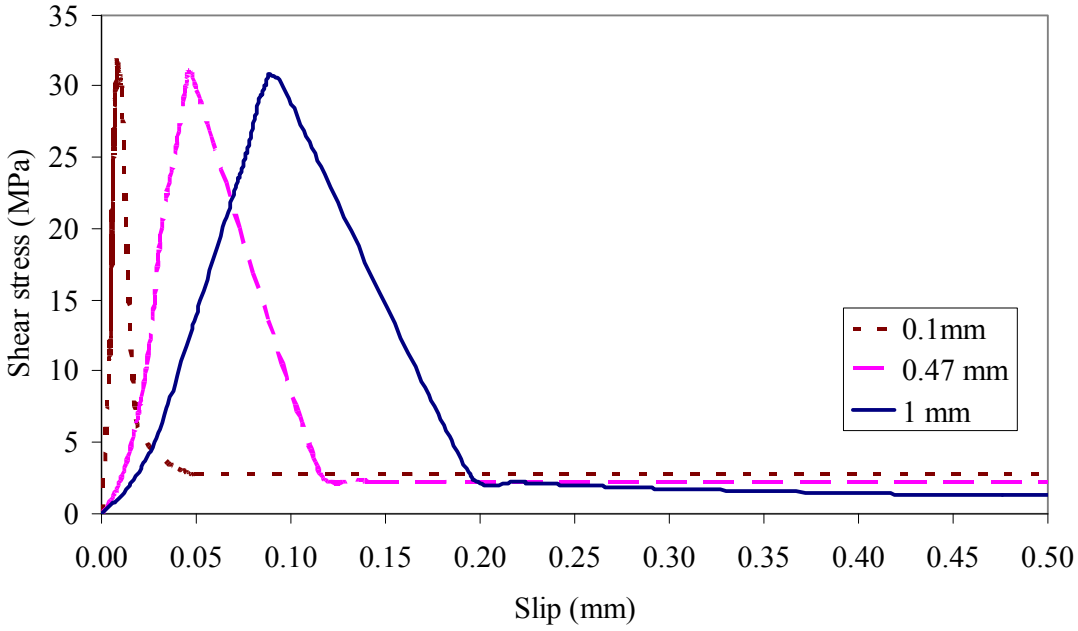

Figure 12 Effect of adhesive thickness on bond-slip response

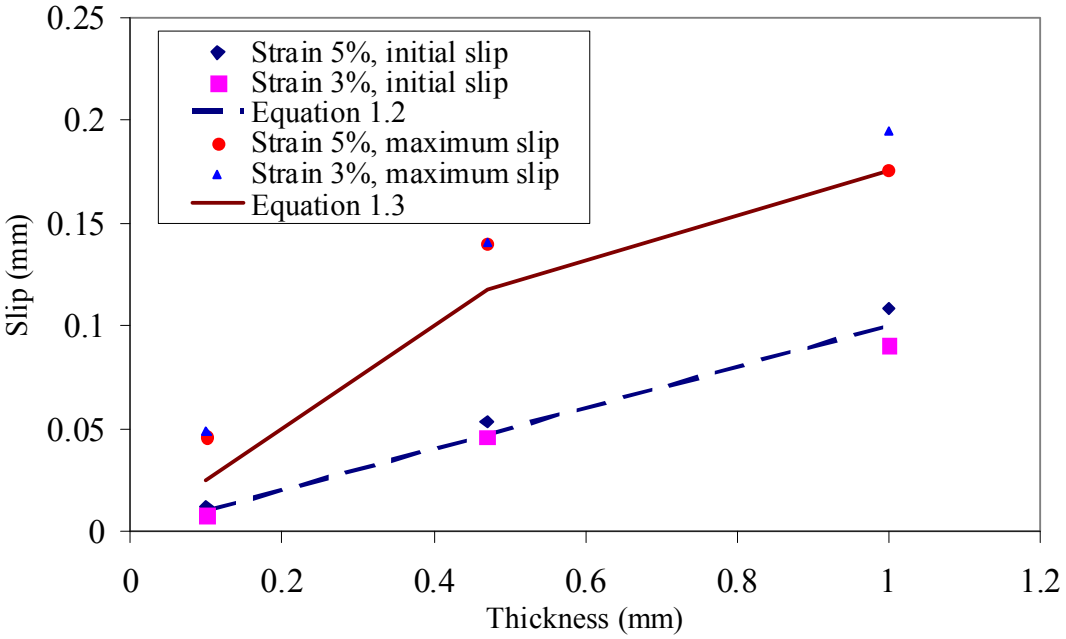

Figure 13 The relationship between slip and adhesive thickness

Table 1 Test configuration of five different series

Series	CFRP Types	CFRP Layers	Steel Thickness mm	Adhesives
1st	Normal Modulus	3	6	Araldite 420
2nd	Normal Modulus	3	6	Araldite 420
3rd	Normal Modulus	3	6	Mbrace saturant & Sikadur 30
4th	Normal Modulus	3	10	Araldite 420, Mbrace saturant & Sikadur 30
5th	High Modulus	5	6	Araldite 420

Table 2 Test results from all series

Specimen Level	Bond length l_1 mm	Ultimate load kN	Failure mode
1st series			
NA250a	250	89.6	Steel adhesive interface debonding and CFRP delamination
NA250b	250	97.2	Steel adhesive interface debonding and CFRP delamination
NA250c	250	77.5	Steel adhesive interface debonding and CFRP delamination
NA250d	250	108.6	Steel adhesive interface debonding and CFRP delamination
NA200a	200	92.6	Steel adhesive interface debonding and CFRP delamination
NA200b	200	71.6	Steel adhesive interface debonding and CFRP delamination
NA200c	200	99.6	Steel adhesive interface debonding and CFRP delamination
NA200d	200	105.0	Steel adhesive interface debonding and CFRP delamination
2nd series			
NA150a	150	99.1	Steel adhesive interface debonding and CFRP delamination
NA150b	150	70.0	Steel adhesive interface debonding and CFRP delamination
NA150c	150	51.4	Steel adhesive interface debonding and CFRP delamination
NA150d	150	91.0	Steel adhesive interface debonding and CFRP delamination
NA80a	80	98.4	Steel adhesive interface debonding and CFRP delamination
NA80b	80	96.9	Steel adhesive interface debonding and CFRP delamination
NA80c	80	69.4	Steel adhesive interface debonding and CFRP delamination
NA80d	80	80.0	Steel adhesive interface debonding and CFRP delamination
3rd series			
NM200a	200	88.2	Steel adhesive interface debonding
NM200b	200	75.5	Steel adhesive interface debonding
NM200c	200	95.2	Steel adhesive interface debonding and CFRP delamination
NS200a	200	75.8	Steel adhesive interface debonding and CFRP delamination
NS200b	200	81.6	Steel adhesive interface debonding and CFRP delamination
NS200c	200	72.9	Steel adhesive interface debonding and CFRP delamination
4th series			
NA200a	200	105.0	Steel adhesive interface debonding and CFRP delamination
NA200b	200	108.0	Steel adhesive interface debonding and CFRP delamination
NM200	200	82.0	Steel adhesive interface debonding
NS200	200	50.0	Steel adhesive interface debonding and CFRP delamination
5th series			
HA200	200	60.0	CFRP rupture

Table 3: Shear stress and slip relationship for three different adhesives

	Maximum shear stress Mpa	Initial slip mm	Maximum slip mm
Araldite 420	30	0.05	0.12
Mbrace saturant	23	0.05	0.12
Sikadur 30	22	0.04	0.1